SPECT/CT registration with the DCC and MC simulations for SPECT imaging

F. Chatelain, L. Desbat, J.F. Moreira, C. Amblard, Vincent Breton

SPECT/CT registration with the DCC and MC simulations for SPECT imaging.

Florent Chatelain, Laurent Desbat, Jean François Moreira, Cécile Amblard, Vincent Breton

Abstract—**We want to perform the attenuation correction in the case of 3D attenuated ray transform with a parallel geometry. We suppose that the attenuation function is available but not registered with the data. We use the sum on each slice of the 2D data consistency conditions of the attenuated Radon transform to register the attenuation function with the data. We then correct for the attenation using the Novikov formula. We show numerical experiments indicating the feasibility of the approach and propose a scheme including the diffusion correction for the registration of CT to SPECT for SPECT imaging improvement.**

Index Terms—**Attenuated Radon Transform, Data Consistency Condition, Tomography, Analytic inversion formula.**

I. INTRODUCTION

Attenuation and diffusion are major problems in SPECT. For improving SPECT images both transmission and emission data can now be jointly acquired on dedicated systems. Thus attenuation and diffusion can be corrected in the activity reconstruction from the SPECT data, see [1], [2], [5]. In this work, we want to improve SPECT reconstructions by the registration of an attenuation model (prior CT exam) with SPECT data using the DCC (Data Consistency Conditions) of the attenuated Radon transform [7], [8]. We suppose in this work that the scattering has been previously corrected, but we propose at the end of the paper how to introduce the scatter correction with MC (Monte Carlo) simulations in an iterative scheme including the presented work. Once the attenuation function has been registered with the data, we compensated for the attenuation in the reconstruction thanks to the Novikov's formula [10].

In the next section we present our notation and we recall the attenuated Radon transform DCC and its use for the attenuation map registration to the emission data (attenuated Radon transform). We also recall the analytical reconstruction of the attenuated Radon transform [9], [10] that we use. In the third section we present numerical experiments indicating that the 3D registration of the attenuation map to emission data (3D attenuated ray transform) is feasible. In the fourth section, we describe a preliminary work on our MC approach for the scattering estimation. We then show how the reconstruction from the attenuated Radon transform, MC simulation for diffusion correction, and the registration of the attenuation map to the

emission data through the DCC optimization could cooperate for the SPECT imaging improvement.

II. DCC AND INVERSION OF THE ATTENUATED RADON TRANSFORM IN 2D

We first recall the definition of the 2D attenuated Radon transform of the function f (the activity) at the angular position $\phi(\in [0, 2\pi[)$ and detector position $u(\in [-1, 1]$ the radius of the activity function support being normalized):

$$g(\phi, u) = R_\mu f(\phi, u) = \int_{L_{\phi,u,v}} e^{-D\mu(x,\zeta)} f(x) dx, \quad (1)$$

with

$$D\mu(x,\zeta) = \int_0^{+\infty} \mu(x + t\zeta) dt$$

and $L_{\phi,u}$ is the line $u\theta + ve_3 + \mathbb{R}\zeta$, with $\theta = (\cos\phi, \sin\phi)$, $\zeta = (-\sin\phi, \cos\phi)$, see figure 1.
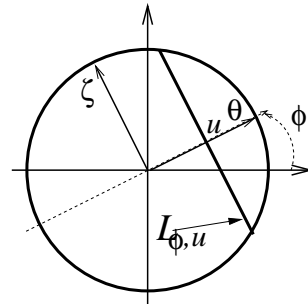

Fig. 1. Geometrical parameters of the problem in 2D

As shown in [9], [10], if μ is known, f can be reconstructed by:

$$f(x_1, x_2) = \frac{1}{4}\Re\left(\text{div}\int_0^{2\pi}\theta e^{D\mu(x,\zeta)}\left(e^{-h}He^h g\right)(\phi, x\cdot\theta)d\phi\right)$$

where $h = \frac{1}{2}(I + iH)R_\mu$, H is the Hilbert transform and R_μ is the 2D attenuated Radon transform.

In this part, we suppose that the attenuation map μ can be estimated from CT scanner data [3] yielding μ_0 and that μ_0 only needs to be registered to the emission data (1). More precisely, we search a transform T from $\mathbb{R}^2$ to $\mathbb{R}^2$, such that
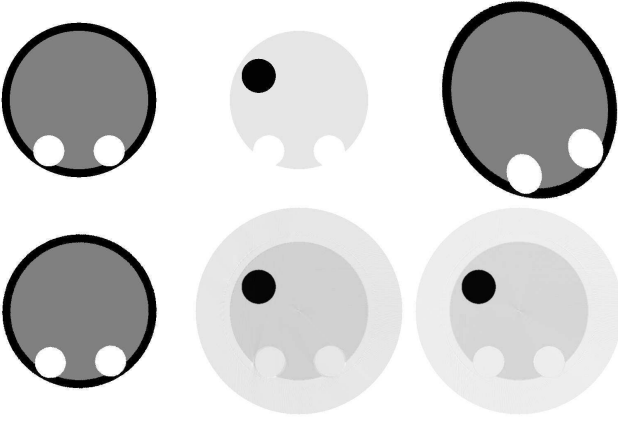
$$\mu_T(x) \stackrel{\text{def}}{=} \mu_0(T(x)) = \mu(x).$$

Fig. 2. First line, left: true attenuation map μ, center: activity map f, right: attenuation model μ_0, second line, left: attenuation map μ_T from the optimized DCC, center: reconstruction with the attenuation map from the optimized DCC, right: reconstruction with the true attenuation map.

Fig. 3. Geometrical parameters of the 3D parallel acquisition.

Following [4], [8], we propose to estimated T from the DCC:

$$\min_T \sum_{k,m} \left(\int_0^{2\pi} \int_{\mathbb{R}} g(\phi,u) u^m e^{\frac{1}{2}(I+iH)R\mu_T(\phi,u)+ik\phi} du d\phi \right)^2$$

where $k \in \mathbb{N}$, $m \in \mathbb{N}$, $0 \le m < k$.

The estimation of μ from the DCC optimization is severly ill conditionned. Thus it is necessary to reduce the degree of freedom of T. We suppose here that T is an affine transform, $Tx = Ax + b$ where A is a 2×2 matrix and $b \in \mathbb{R}^2$, thus only 6 parameters need to be estimated. In practice, it would mean that we want to register the attenuation map (from a CT) to emission data (SPECT) including the different scales of the imaging systems. We restrict the sum in the DCC over $0 \le m < k \le P$, P integer being chosen small (here equal to 2). We show in figure 2 simulation results in 2D, including 2D reconstruction with the Navikov formula. These results are similar to those obtained in [4], [8]. The DCC allows for a sufficiently good estimation of the affine transform in order to provide a reconstructed image essentially as good as those obtained with the true attenuation.

III. 3D REGISTRATION OF THE ATTENUATION MAP TO THE EMISSION DATA

In this part, we consider a classical parallel SPECT trajectory, where the data coordinates are the angle $\phi \in [0; 2\pi[$ of the γ-camera and the $(u,v) \in \mathbb{R}^2$ coordinates of the pixels on the γ-camera along the axis $\theta = (\cos\phi, \sin\phi, 0)$ and $e_3 = (0,0,1)$, see figure 3.

We consider that the SPECT emission data d contains two types of contributions: the direct contributions g modeled by the attenuated Radon transform and the diffusion data d_d. Thus

$$d(\phi,u,v) = g(\phi,u,v) + d_d(\phi,u,v)$$

with

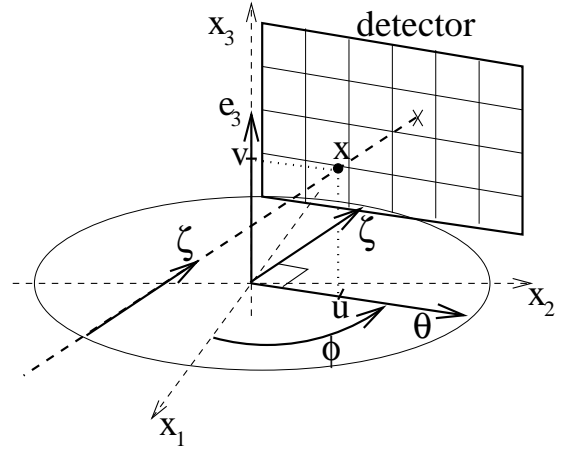$$g(\phi,u,v) = \int_{L_{\phi,u,v}} e^{-D\mu(x,\zeta)} f(x) dx,$$

with

$$D\mu(x,\zeta) = \int_0^{+\infty} \mu(x+t\zeta) dt$$

and $L_{\phi,u,v}$ is the line $u\theta + ve_3 + \mathbb{R}\zeta$, $\zeta = (-\sin\phi, \cos\phi, 0)$, f is the 3D activity function and μ is the 3D attenuation function.

We suppose here that d_d can be estimated (by MC simulation for example) and corrected. Thus if μ is known, as in the previous section, f can be reconstructed by slice by slice, i.e., at fixed v by the Novikov formula:

$$f(x) = \frac{1}{4} \Re \left(div \int_0^{2\pi} \theta_v e^{D\mu(x,\zeta)} \left(e^{-h} H e^h g_v \right)(\phi, x \cdot \theta) d\phi \right)$$

where $x = (x_1, x_2, v)$, $g_v(\phi,u) = g(\phi,u,v)$, (note that $f(x) = f(x_1,x_2,v) = f_v(x_1,x_2)$) $\theta_v = (\cos\phi, \sin\phi)$. As in section II, $h = \frac{1}{2}(I+iH)R_\mu$, H is the Hilbert transform and R_μ is the 2D attenuated Radon transform, i.e., $R_\mu f_v(\phi,u) = g(\phi,u,v)$. In our parallel geometry, the 3D reconstruction is thus classically reduced to a 2D reconstruction at fixed v.

Just as in section II, we suppose that the attenuation map μ_0 can be estimated from CT scanner data [3] and that it only needs to be registered to the emission data g (SPECT). More precisely, we search a transform T from $\mathbb{R}^3$ to $\mathbb{R}^3$, e.g. a rigid transform given by a rotation matrix ρ (driven by 3 parameters) and a translation t such that

$$\mu_T(x) \overset{\text{def}}{=} \mu_0(T(x)) \overset{\text{def}}{=} \mu_0(\rho(x) + t) = \mu(x)$$

Just as in the previous section, we propose to estimated T, thus here ρ and t, from the DCC. They are here computed slice by slice and accumulated:

$$\min_{\rho,t} \sum_v \sum_{k,m} \left(\int_0^{2\pi} \int_{\mathbb{R}} g_v(\phi,u) u^m e^{\frac{1}{2}(I+iH)R\mu_T(\phi,u)+ik\phi} du d\phi \right)^2$$

where $0 \le m < k \le P$, P integer being chosen small (here equal to 2).

We show in figures 4 and 5 simulation results in 3D. We have optimized the registration parameters, i.e. the 3D rotation ρ and the 3D translation t (globally 6 parameters), such that $\mu_{\rho,t}(x) = \mu_0(\rho(x) + t)$ minimizes the DCC.
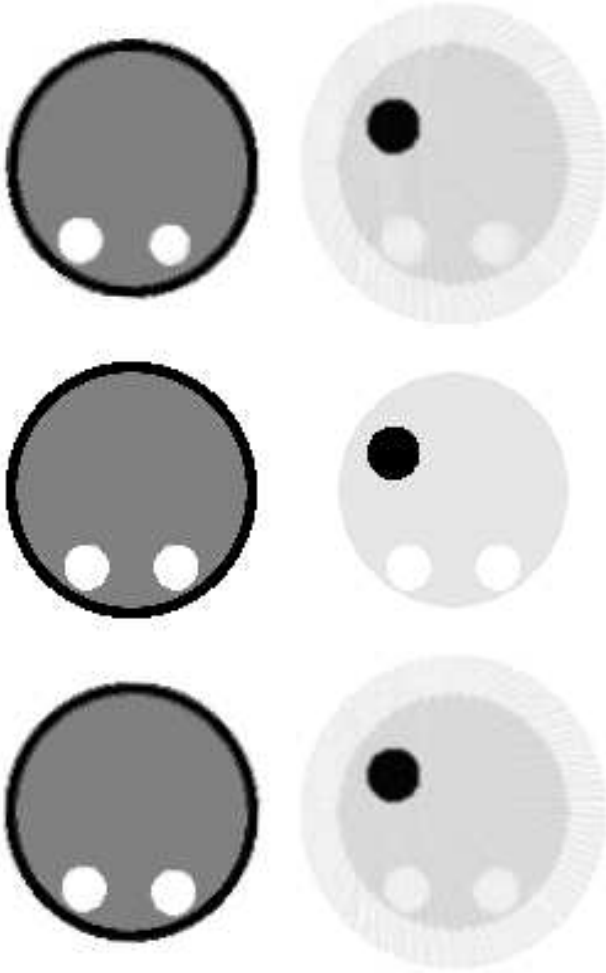
Fig. 4. 3D registration of the attenuation function and 3D reconstruction with attenuation compensation ; slice $v = .516$. First line: left: model attenuation map μ_0 (3D rotation of the true attenuation with rotation Euler angles in radian equal to $(\pi/64; \pi/80; -\pi/68))$; right: activity reconstructed from the Nivikov formula with the model attenuation μ_0. Second line: left: true attenuation map μ ; right: true activity.Third line: left: attenuation map μ_T from the optimized DCC ; rigt: activity reconstructed with the attenuation μ_T.
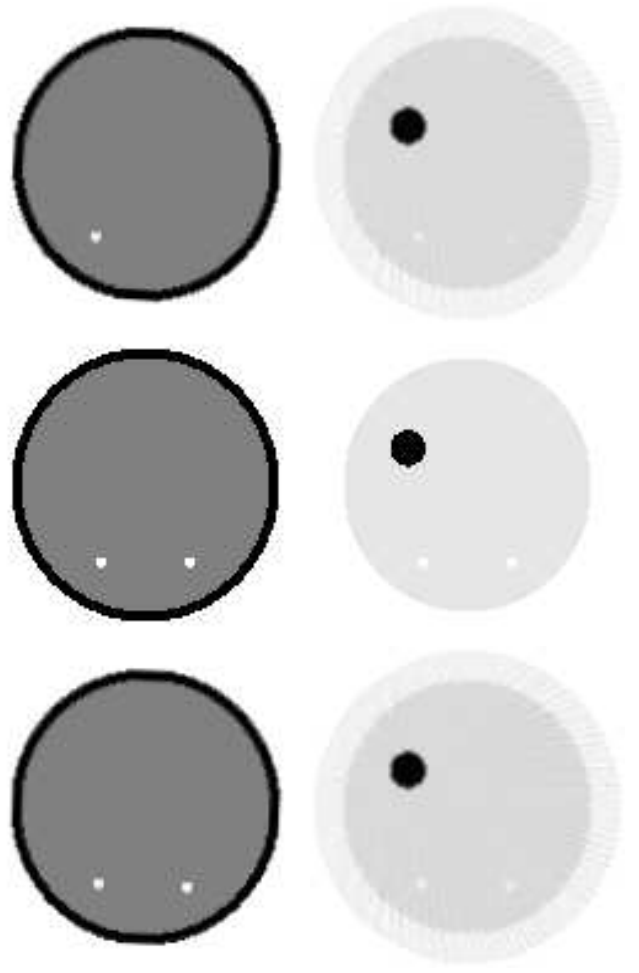
Fig. 5. 3D registration of the attenuation function and 3D reconstruction with attenuation compensation ; slice $v = .42$. First line: left: model attenuation map μ_0; right: activity reconstructed from the Nivikov formula with the Model attenuation μ_0. Second line: left: true attenuation map μ ; right: true activity.Third line: left: attenuation map μ_T from the optimized DCC ; rigt: activity reconstructed with the attenuation map μ_T.

Our 3D activity phantom is composed by a spherical background activity of 125 on the centered sphere of radius .893 ; three spheres of null activity, respectively centered at (.6,0,-.285), (.48,.285,.57), (.48,-.285,.57), of respective radius .285, .152 and .152 ; two high activity (1250) spheres respectively centered on (-.228,-.38,.551) and (.532,.19,.323) and of respective radius .171 and .057.

Our 3D attenuation map μ is composed by a centered spherical shell of radius .893 to .95 of attenuation 4 ; a centered sphere of radius .893 of attenuation 2 ; three spheres of null attenuation (the same as the spheres of null activity) respectively centered at (.6,0,-.285),(.48,.285,.57), (.48,-.285,.57), of respective radius .285, .152 and .152. The model attenuation μ_0 is a rotation of μ with a matrix of Euler angles in radian $(\pi/64; \pi/80; -\pi/68)$.

The figure 4 show the slice $v = 0.516$, thus close to the center of the null activity spheres centered at (.48,.285,.57) and (.48,-.285,.57). The figure 5 show the slice $v = 0.42$, thus close to the bottom of the null activity spheres centered at (.48,.285,.57) and (.48,-.285,.57). In both figures, the DDC minimization improves the registration of the attenuation, i.e., $\mu_{\rho,t}$ is closer to μ than the original model μ_0 is. Using the Nivikov formula, the reconstruction slices with $\mu_T = \mu_{\rho,t}$ have less artefacts compare to thoses with μ_0. In particular, in figure 5, both null activity small discs at the bottom (sphere cross sections) can be seen in the reconstruction with the Novikov formula using $\mu_{\rho,t}$ whereas one disapears in the reconstruction from μ_0.

IV. PERSPECTIVES AND DISCUSSION

A. SPECT diffusion correction with MC

Efficient Monte Carlo methods are used in SPECT associated with statistical reconstruction techniques to compensate for scatter, see [2]. In our work, we could use a Monte Carlo approach only for the scattering estimation, in order to correct

the data before the DCC computation. We tested a Monte Carlo simulator based on the GATE plateform (GEANT4 Application for Tomographic Emmission), itself based on the GEANT4, see [6], [11]. GEANT4, developed by the nuclear science community, offers general codes of particule simulations. The GATE package is dedicated to tomography. It is used for the simulation of SPECT (source, attenuation, gamma-camera, etc.) Within the simulation, we can separate the direct contribution from the scattering part. In the figure 6 we show the phantom that we have used and the MC simulations obtained with GATE.
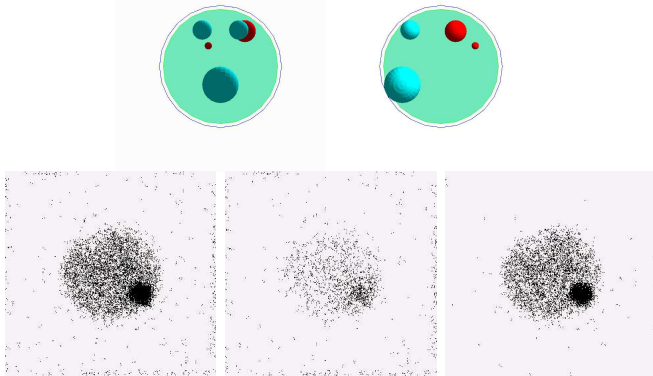
Fig. 6. First line: two views of our Phantom composed by a spherical shell of bone attenuation, inside of the sphere is water with relatively low emission of 99mTC ($5,410^6$ Bq but only one second of activity is simulated). We have also three balls of air with no emmission and two balls with high emmision (1 250 Bq/mm^3). The attenuation value are taken from the GEANT4 data base. Second line. left: data d ; center: diffusion d_d, right: projection data g with diffusion correction simulations of raw data d (left), corresponding scatter data d_d (center) and corrected data g (projection at angle $\phi = 0$).

B. MC and DCC cooperation for SPECT reconstruction

Our idea is to estimate the activity from SPECT data (roughly corrected from diffusion) and an initial registration of CT to SPECT. Then we want to correct for the diffusion with MC simulations. From the corrected data we improve the registration thanks to the DCC. We iterate on that scheme of estimation of the activity, prediction and correction of the diffusion with MC, registration improvement with the DCC. The major practical interest of this approach is that it does not need dedicated integrated SPECT/CT systems but only classical imaging systems (SPECT and CT).

We propose in figure 7 an iterative algorithm in order to reconstruct an activity map f from emission SPECT measures g and an attenuation CT map μ_0. We assume that we have a prior idea of the rigid transform T_1 which must be applied on the attenuation map in order to register the activity and attenuation maps. It is then possible to reconstruct a first activity map f_1 from the registrated attenuation $\mu_1 = \mu_0 \circ T_1$ and from the basically corrected diffusion data g_1, by inversion of the attenuated Radon transform. The MC method can simulate diffusion data $d_{d,2}$ from f_1 and μ_1. From new corrected data $g_2 = d - d_{d,2}$, the DCC allow to estimate a new rigid transfomation T_2. A

new activity map is estimated from $\mu_2 = \mu_0 \circ T_2$ and g_2 by the inversion of the attenuated Radon transform, etc. The algorithm stop when T does not change significantly.

The perspective of our work is to develop and test such an iterative method coupling MC simulations and DCC for SPECT/CT registration and SPECT imaging improvement based on this algorithm.
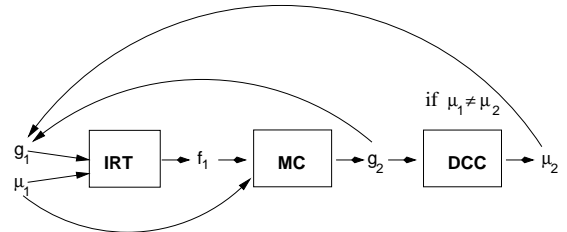
Fig. 7. Scheme of our algorithm. IRT is the Inversion of the attenuated Radon Transform (with the Novikov formula or more realistically with algebraic technics including geometrical and partial volume effects), MC is a Monte Carlo simulator, DCC is the Data Consistency Conditions optimization method.

REFERENCES

[1] D.L. Baily et al Improved SPECT using simultaneous emission and transmission tomography *J. of Nucl. Med.*, 28, pp. 2263–2274, 1987.

[2] F.J. Beekman, et al, Efficient fully 3-D iterative SPECT reconstruction with Monte Carlo-based scatter compensation, IEEE *Trans. Med. Imag.*, Vol. 21, No. 8, pp. 867–877, 2002.

[3] S.C. Blankespoor et al Attenuation correction of spect using x-ray ct on an emission -transmission ct system: Myocardial perfusion assessment. *IEEE TNS*, 43:2263–2274, 1996.

[4] R. Faghihi and L. Desbat Experiments on the DCC for SPECT and CT data registration. *IEEE NSSMIC conference*, 2001.

[5] B.H. Hasegawa et al Object specific attenuation correction of SPECT with corrected dual-energy X-ray CT. *IEEE TNS*, 40:1242–1252,1993.

[6] D. Lazaro, et al, Validation of the GATE Monte Carlo simulation platform for modelling a CsI(Tl) scintillation camera dedicated to small animal imaging, *Phys. Med. Biol.*, 49, pp. 271–85, 2004.

[7] C. Mennessier, F. Noo, R. Clackdoyle, G. Bal, and L. Desbat. Attenuation correction in SPECT using consistency conditions for the exponential ray transform. *Phys. Med. Biol.*, 44, pp. 2483–2510, 1999.

[8] F. Natterer. Determination of tissue attenuation in emission tomography of optically dense media. *Inverse Problems*, 9(6):731–6, 1993.

[9] F. Natterer. Inversion of the attenuated radon transform. *Inverse problems*, 17:113–119, 2001.

[10] R.G. Novikov. An inversion formula for the attenuated x-ray transform. *preprint*, UMR CNRS 6629, département de mathématiques, université de Nantes, 2000.

[11] G. Santin, et al, A Geant4-based simulation platform for PET and SPECT integrating movement and time management, *IEEE Trans. Nucl. Sci.*, 50, pp. 1516–1521, 2003